Ms. for *Organometallics* (ARTICLE)

$[MnBrL(CO)_4]$ (L = Amidinatogermylene): Reductive Dimerization, Carbonyl Substitution, and Hydrolysis Reactions

Javier A. Cabeza,[*†] *Pablo García-Álvarez,*[*†] *Roberto Gobetto,*[‡] *Laura González-Álvarez,*[†] *Carlo Nervi,*[‡] *Enrique Pérez-Carreño,*[§] *and Diego Polo*[†]

[†]Departamento de Química Orgánica e Inorgánica-IUQOEM, Centro de Innovación en Química Avanzada (ORFEO-CINQA), Universidad de Oviedo-CSIC, E-33071 Oviedo, Spain

[§]Departamento de Química Física y Analítica, Universidad de Oviedo, E-33071 Oviedo, Spain

[‡]Dipartimento di Chimica, Università di Torino, via P. Giuria 7, 10125 Torino, Italy

*E-mail: jac@uniovi.es (J.A.C.) and pga@uniovi.es (P.G.-A.)

ABSTRACT: The manganese(I) carbonyl complex [MnBr{Ge(^{i}Pr$_2$bzam)^{t}Bu}(CO)$_4$] (**1**; ^{i}Pr$_2$bzam = 1,3-di(isopropyl)benzamidinate), which contains an amidinatogermylene ligand, reacts with LiPh or Li^{t}Bu at room temperature undergoing a reductive dimerization process that leads to the manganese(0) dimer [Mn$_2${Ge(^{i}Pr$_2$bzam)^{t}Bu}$_2$(CO)$_8$]. This complex and the monosubstituted derivative [Mn$_2${Ge(^{i}Pr$_2$bzam)^{t}Bu}(CO)$_9$] have also been prepared by reacting [Mn$_2$(CO)$_{10}$] with Ge(^{i}Pr$_2$bzam)^{t}Bu at high temperature (110 ºC). These binuclear complexes contain their germylene ligands in axial positions (*trans* to the Mn–Mn bond). The large volume of the germylene ligand clearly affects the reactivity of complex **1** with neutral 2-electron donor reagents, since for bulky reagents, the CO-substitution occurs *trans* to the germylene ligand, as in *trans-mer*-[MnBrL{Ge(^{i}Pr$_2$bzam)^{t}Bu}(CO)$_3$] (L = Ge(^{i}Pr$_2$bzam)^{t}Bu, PMe$_3$), whereas for small reagents, the CO-substitution occurs *cis* to the germylene ligand, as in *fac*-[MnBr(CN^{t}Bu){Ge(^{i}Pr$_2$bzam)^{t}Bu}(CO)$_3$]. The IR spectra (ν_{CO}) of these complexes have confirmed that the germylene Ge(^{i}Pr$_2$bzam)^{t}Bu is a very strong electron-donating ligand, even stronger than the most basic trialkylphosphanes and N-heterocyclic carbenes. The hydrolysis of complex **1** leads to the salt [^{i}Pr$_2$bzamH$_2$][MnBr{Ge(OH)$_2$^{t}Bu}(CO)$_4$], the anion of which contains an unprecedented germanato(II) ligand, [Ge(OH)$_2$^{t}Bu]$^-$, in *cis* to the Br atom. This hydrolysis product and its precursor **1** have been tested as catalyst precursors for the electrolytic reduction of CO_2, showing no significant activity.

INTRODUCTION

Many transition metal (TM) complexes containing heavier tetrylenes (HTs, compounds having a heavier group 14 atom in the +2 oxidation state) as ligands have been prepared and characterized in the last 40 years, but its derivative chemistry (stoichiometric or catalytic) has still been little investigated.[1,2] This can be attributed, among other factors, to the general low stability of HT–TM complexes towards oxidation,[3] hydrolysis,[4] and/or HT ligand displacement.[5] Fortunately, the HT–TM chemistry has been recently boosted by the appearance of amidinato-HTs in the coordination chemistry arena.[2b] In fact, although the first transition metal complex containing an amidinato-HT ligand was reported only seven years ago,[6] this family of complexes already contains over one hundred members[2b,7] and some of them have already been used as active catalysts for important transformations of organic substrates.[8] The fact that (a) both the electronic and steric characteristics of amidinato-HTs, E(R^{1}NCR^{2}NR^3)X (E = Si, Ge, or Sn), can be easily and extensively tuned (many different combinations of E, R^1, R^2, R^3, and X are

possible) and (b) that they have proven to be even stronger electron-donating ligands than NHCs,[2b] alleviating some of the stability issues associated to the general HT ligand lability,[5,9] accounts for the rapid expansion of the coordination chemistry of these compounds.[2b]

In this context, by using the very bulky amidinatogermylene Ge(^{i}Pr$_2$bzam)^{t}Bu (**A**; ^{i}Pr$_2$bzam = 1,3-di(isopropyl)benzamidinate), we have recently described the synthesis of [MnBr{Ge(^{i}Pr$_2$bzam)^{t}Bu}(CO)$_4$] (**1**) (Scheme 1),[4b] which is the only specimen of the large family of complexes of the type [MnXL$_n$(CO)$_{5-n}$] (X = halogen)[10] in which L is an HT ligand. We have also shown that its terminal amidinatogermylene ligand can be transformed, upon reaction with Ag[BF$_4$] or LiMe (but not with AgOTf, OTf = triflate), into an unprecedented κ^2*N*,*Ge*-iminegermanato(II) ligand that chelates the metal atom and that contains the X group attached to the Ge atom (Scheme 1).[4b]

Scheme 1[a]

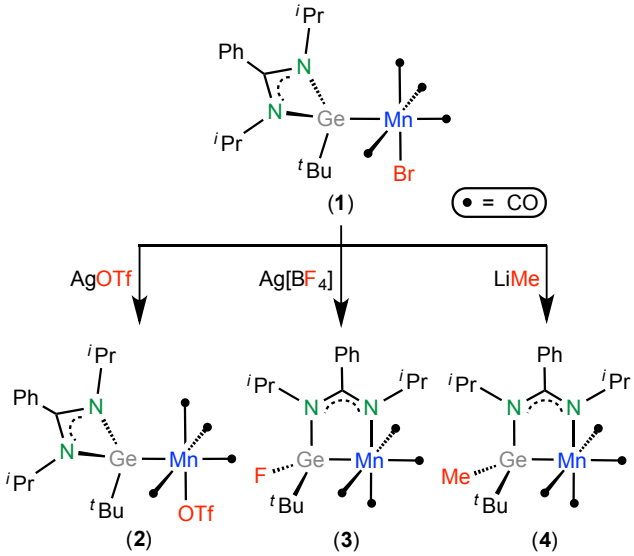

[a]Reported[4b] reactivity of [MnBr{Ge(^{i}Pr$_2$bzam)^{t}Bu}(CO)$_4$] (**1**) with anionic nucleophiles.

Continuing with our investigations on the derivative chemistry of HT–TM complexes,[4b,11] we now describe reactions of complex **1** with other nucleophiles, neutral and anionic, including water. These reactions have shown that, (a) when treated with LiPh or Li^{t}Bu, complex **1** can undergo a reductive dimerization process that leads to a binuclear manganese(0) derivative, (b) the large volume of the amidinatogermylene ligand affects the reactive coordination sites of **1** in CO substitution processes, and (c) in the presence of moisture, a hydrolysis product, which contains a novel alkyldihydroxogermanato(II) ligand, [Ge(OH)$_2$^{t}Bu]$^-$, and that can be postulated as an early-stage intermediate in the hydrolytic degradation of amidinato-HT complexes, has been obtained.

Additionally, having in mind the important role that substituted carbonyl manganese(I) complexes are currently playing as electrocatalysts for the reduction of CO_2,[12] we have also evaluated the potential of complex **1** and its hydrolysis product in this cataltic process. Theoretical DFT calculations have helped rationalize some of the experimental results

RESULTS AND DISCUSSION

Reactions of Complex 1 with LiPh and Li^{t}Bu. Both reagents behaved similarly in their reactions with complex **1**. An excess of the lithium reagent was necessary to complete the consumption of complex **1** (IR monitoring of the reaction solution, ν_{CO} region). In both cases, no trace of a transmetalation derivative similar to complexes **2**–**4** was observed and a chromatographic workup of the reaction mixture allowed the isolation of the dimeric manganese(0) derivative $[Mn_2\{Ge(^i Pr_2bzam)^t Bu\}_2(CO)_8]$ (**5**) in moderate yield (Scheme 2). Therefore, these reactions are redox processes in which the LiX reagent (X = Ph, ^{t}Bu) acts as reducing agent. The formation of **5** can be explained as a result of the homolytic cleavage of the Mn–X bond of a transient transmetallation derivative, $[MnX\{Ge(^i Pr_2bzam)^t Bu\}(CO)_4]$, followed by recombination of the resulting radicals to give **5** and X–X. Although the transmetallation derivatives could not be detected, their participation in the process is likely, because (a) a GC-MS analysis of the reaction solution confirmed the presence of biphenyl in the case of the reaction involving LiPh and (b) it has been reported that the transient complex [Mn(η^1-fluorenyl)$(CO)_5$], prepared from $[MnBr(CO)_5]$ and fluorenyllithium, evolves toward [Mn(η^5-fluorenyl)$(CO)_3$], $[Mn_2(CO)_{10}]$, and 9,9'-bifluorene.[13] All attempts (GC-MS and NMR analyses) to confirm the presence of 2,2,3,3-tetramethylbutane as a putative oxidation product in the reaction that used Li^{t}Bu were unsuccessful. In fact, it has been reported that glass or solvent hydrogen sources can trap the ^{t}Bu radical.[14] This reductive dimerization also occurs in the reaction of **1** with LiMe, since the presence of a small amount of dimer **5** in the reaction mixture has now been identified by IR spectroscopy, although the major product of this reaction is the chelated complex **4** (Scheme 1).[4b]

Scheme 2

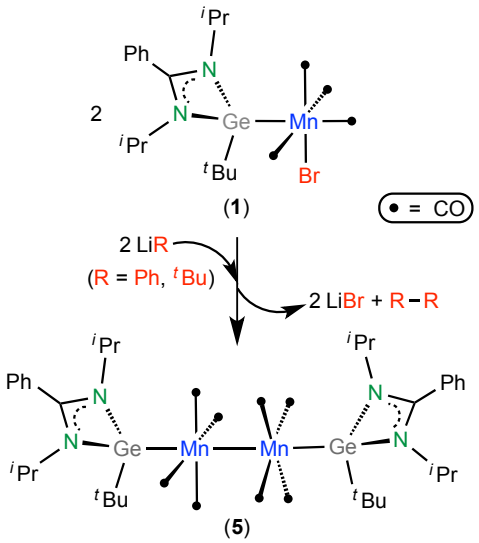

The structure of complex **5** was determined by X-ray diffraction (XRD) (Figure 1). The molecule, which has an approximate (non-crystallographic) C_2 symmetry, can be described as a formal derivative of $[Mn_2(CO)_{10}]$ in which two Ge(^{i}Pr$_2$bzam)^{t}Bu germylenes have replaced the two axial CO ligands. To minimize steric interactions, the CO ligands are arranged in a staggered conformation and the Ge1–C14 (or Ge2–C31) and Ge1–C4 (or Ge2–C21) bonds of the germylenes are roughly eclipsed with two CO ligands because this conformation results in the greatest separation between the CO ligands and the benzamidinato *iso*-propyl groups. Related doubly axially-substituted structures have been reported for a few $[Mn_2L_2(CO)_8]$ complexes (L = *P*-donor ligand).[15]

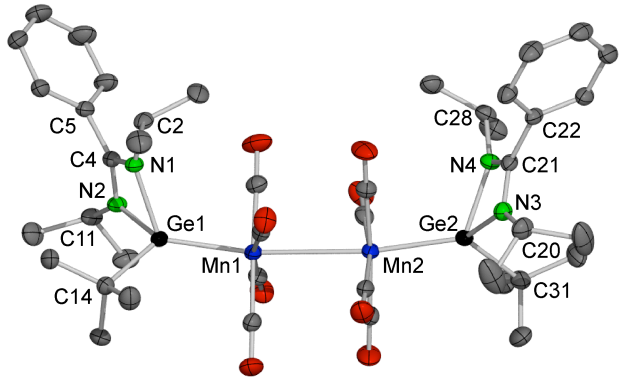

Figure 1. XRD molecular structure of **5** (35% displacement ellipsoids; H atoms omitted for clarity). Selected bond lengths (Å) and angles (deg): Mn1−Mn2 2.8690(7), Mn1−Ge1 2.3271(6), Ge1−C14 1.999(4), Ge1−N1 1.998(2), Ge1−N2 1.982(3), N1−C2 1.474(4), N1−C4 1.324(4), N2−C4 1.328(4), N2−C11 1.465(4), C4−C5 1.488(4), Mn2−Ge2 2.3222(6); Mn1−Ge1−N1 116.97(8), Mn1−Ge1−N2 121.23(9), C14−Ge1−Mn1 127.2(1), C14−Ge1−N1 103.6(1), C14−Ge1−N2 105.0(1), N1−Ge1−N2 65.9(1), Ge1−N1−C4 92.0(2), Ge1−N2−C4 92.6(2), N1−C4−N2 109.5(3), Ge1−Mn1−Mn2 169.87(2), Ge2−Mn2− Mn1 172.48(2).

With the aim of rationalizing these results in conjunction with those displayed in Scheme 1, we decided to calculate by DFT methods, for each X^- reagent (X = Ph, ^{t}Bu, Me, Br, OTf), the thermodynamic stability (Gibbs energy) of the products of the reactions shown in Scheme 3, which, starting from **1** and X^- can lead to the direct transmetallation complexes [MnX{Ge(^{i}Pr$_2$bzam)^{t}Bu}(CO)$_4$] (eq. 1), to the chelated products [Mn{κ^2*N*,*Ge*-GeX(^{i}Pr$_2$bzam)^{t}Bu}(CO)$_4$] (eq. 2), or to the products of the reductive dimerization processes, **5** and X_2 (eq. 3).

Scheme 3. DFT-Studied Reactions

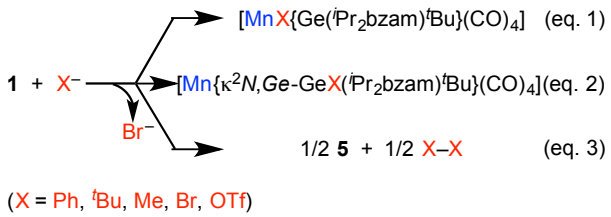

Table 1. Relative Gibbs Energies of the Reaction Products of Eq. 1–3 of Scheme 3[a]

Eq.	Reaction Product(s)	X = Ph	X = ^{t}Bu	X = Me	X = Br	X = OTf
1	[MnX{Ge(^{i}Pr$_2$bzam)^{t}Bu}(CO)$_4$]	0.0	0.0	0.0	0.0	0.0
2	[Mn{κ^2*N*,Ge-GeX(^{i}Pr$_2$bzam)^{t}Bu}(CO)$_4$]	–4.6	–10.8	–12.7	1.3	23.5
3	½ **5** + ½ X–X	–14.3	–25.7	–16.6	37.2	44.6

[a] ΔG_{298} (kcal mol^{-1}) calculated in toluene (CPCM model) at the wB97XD/cc-pVDZ (SDD for Mn and Ge) level of theory.

Table 1 shows that, for X = Ph, ^{t}Bu, and Me, the reactions represented by eq. 1 are thermodynamically disfavored with respect to the reactions represented by eqs. 2 and 3, and that, for X = Ph and ^{t}Bu, the redox processes (eq. 3) are clearly more favorable than the formation of the chelated products (eq. 2). However, for X = Me, the difference between the redox (eq. 3) and the chelation (eq. 2) processes is only 3.9 kcal mol^{-1}. These thermodynamic calculations provide a rationale as to why [MnX{Ge(^{i}Pr$_2$bzam)^{t}Bu}(CO)$_4$] and [Mn{κ^2*N*,Ge-GeX(^{i}Pr$_2$bzam)^{t}Bu}(CO)$_4$] have not been experimentally observed for X = Ph and ^{t}Bu (in these cases eq. 3 is the most favorable process) and why both products of eqs. 2 and 3 have indeed been observed for X = Me, but they cannot explain why the chelated methyl complex **4** is by far the major product of the reaction of complex **1** with LiMe. Regarding this fact, the X-ray structure of complex **4**, which contains a chelating κ^2*N*,Ge-

iminegermanato(II) ligand that formally arises from the addition of the Me^- nucleophile to the Ge atom of complex **1**, revealed some steric congestion around the Ge-bound Me group, mostly provoked by the nearby ^{t}Bu and ^{i}Pr groups.[4b] Therefore, the different reactivity of complex **1** with LiMe, with respect to that observed for LiPh and Li^{t}Bu, should have a kinetic origin, probably related to the smaller volume of the Me group with respect to those of the Ph and ^{t}Bu groups.

Table 1 also shows that complex **1** is only a bit more stable than the elusive chelated derivative [Mn{κ^2*N*,Ge-GeBr(^{i}Pr$_2$bzam)^{t}Bu}(CO)$_4$]. As no trace of the latter was observed when complex **1** was heated in toluene at 90 ºC for 30 min (higher temperatures led to extensive decomposition), the transformation of **1** into [Mn{κ^2*N*,Ge-GeBr(^{i}Pr$_2$bzam)^{t}Bu}(CO)$_4$] should be kinetically hampered, at least at mild temperatures. The much greater thermodynamic stability of [Mn(OTf){Ge(^{i}Pr$_2$bzam)^{t}Bu}(CO)$_4$] (**2**) with respect to the products of eqs. 2 and 3 for X = OTf justifies that this complex is the only product of the reaction of complex **1** with AgOTf (Scheme 1).[4b]

To shed additional light on the redox process that leads to complex **5** and to investigate the purported electrocatalysis towards the reduction of carbon dioxide, we studied the electrochemical properties of complex **1**. The cyclic voltammogram of complex **1** in acetonitrile (Figure 2) shows the typical electrochemical behaviour of bromocarbonylmanganese complexes, since it undergoes two chemical irreversible reductions, at the peak potentials of –1.53 V (R1) and –1.73 V (R2), and a single reoxidation, at –0.63 V (O1) (vs. Ag/AgCl). These electrochemical processes are straightforwardly assigned to: a) reduction of **1**, fast dissociation of the Br^- anion (R1) and quick formation of the Mn–Mn bonded dimer **5**, b) reduction of the *in situ* formed dimer **5** (R2), and c) oxidation of dimer **5** (O1), in a similar way as that previously observed for [MnBr(bpy)(CO)$_3$] (bpy = 2,2'-bipyridine).[12b]

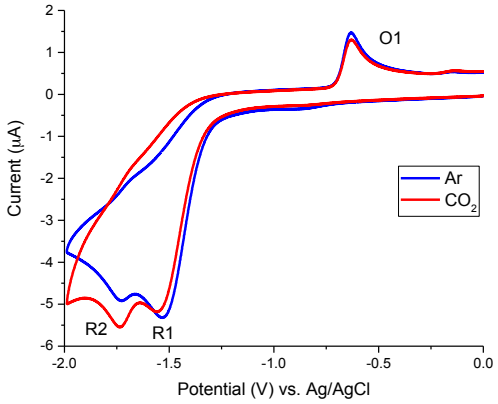

Figure 2. CVs of a 1 mM solution of **1** in acetonitrile at 0.2 V s^{-1} under Ar (blue) and under CO_2 (red).

An analysis of the frontier molecular orbitals of **1** nicely rationalizes the behavior of this complex under reducing conditions, since its LUMO has a great contribution from the Br atom and the Mn–Br overlap is clearly antibonding (Supporting Information, Figure S8).[4b] Therefore, upon 1 electron reduction, the reduced species $[MnBr\{Ge(^{i}Pr_2bzam)^{t}Bu\}(CO)_4]^{-\cdot}$ is prone to release a Br^- anion and the resulting neutral radical $[Mn\{Ge(^{i}Pr_2bzam)^{t}Bu\}(CO)_4]^{\cdot}$ rapidly forms the dimer **5**.

Figure 1 also shows that there are no significant differences between the CVs of complex **1** under Ar and under CO_2. Therefore, complex **1** is not an active electrocatalyst for the reduction of CO_2 in neat acetonitrile. A similar situation has been reported for manganese carbonyl bpy derivatives that, interestingly, are very active for the electrochemical reduction of CO_2 if a Brønsted acid is added to the solution[12b] or a local proton source exists in the catalyst precursor.[12a,12f] Addition of water (5 %) as Brønsted acid to an acetonitrile solution of **1** decomposed the complex and the reduction peak shifted from –1.53 to –1.89 V (vs. Ag/AgCl) (Supporting Information, Figure S9). However, as a small current increase was observed in the CV after the acetonitrile/water solution was saturated with CO_2 (Supporting Information, Figure S9), we decided to perform an exhaustive electrolysis at a potential of –1.90 V with the aim of getting insights into the electrocatalytic behavior. Monitoring by gas chromatography the amount of H_2 and CO produced under a constant flow of CO_2 (8.67 mL min^{-1}) unfortunately revealed that **1** is not an active catalyst for the reduction of CO_2 under these conditions, (Supporting Information, Figures S10 and S11), since the TON of CO produced after 140 min reached a value of only 0.97, whereas the TON of H_2 was only 3.30.

With the aim of checking whether complex **5** could also be prepared directly from $[Mn_2(CO)_{10}]$, we treated this reagent with two equivalents of $Ge(^{i}Pr_2bzam)^{t}Bu$ (**A**) in toluene at reflux temperature. The monosubstituted derivative $[Mn_2\{Ge(^{i}Pr_2bzam)^{t}Bu\}(CO)_9]$ (**6**) was initially formed (Scheme 4), but the long reaction time (7 h) required to observe its complete consumption (IR monitoring of the reaction solution, ν_{CO} region) and the high reaction temperature (110 ^{o}C) led to extensive decomposition and complex **5** was isolated in only a 20% yield after a chromatographic workup. In a separate experiment we isolated the monosubstituted derivative **6** in good yield (71 %) by treating complex **1** with one equivalent of germylene **A** in toluene at reflux temperature for 4 h. These results totally differ from those reported by the groups of Roesky and Stalke for reactions of $[Mn_2(CO)_{10}]$ with the amidinatosilylenes $Si(^{t}Bu_2bzam)X$ ($^{t}Bu_2bzam$ = 1,3-di(tertbutyl)benzamidinato; X = Cl, NPh_2), which gave the disproportionation salts $[Mn(CO)_4\{Si(^{t}Bu_2bzam)X\}_2][Mn(CO)_5]$.[16]

Scheme 4

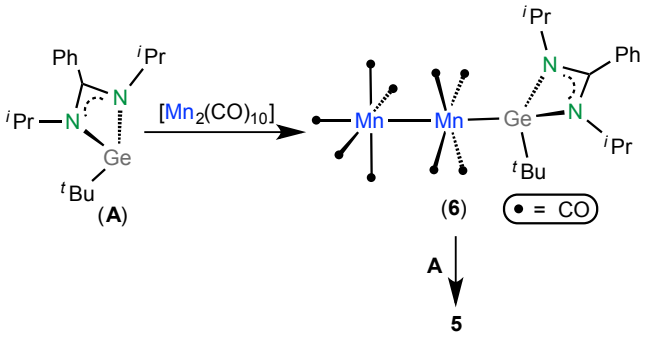

The XRD structure of complex **6** (Figure 3) confirms the substitution of germylene **A** for an axial CO ligand of $[Mn_2(CO)_{10}]$. To minimize steric interactions, as described above for the XRD structure of **5**, complex **6** also has a staggered conformation of the CO ligands and an eclipsed arrangement of the Ge1–C14 and Ge1–C4 vectors with two CO ligands. Related structures have been reported for a few $[Mn_2L(CO)_9]$ complexes in which L is a bulky *P*-donor ligand;[17] however, when L is smaller, the substitution may occur at an equatorial position.[15e,18]

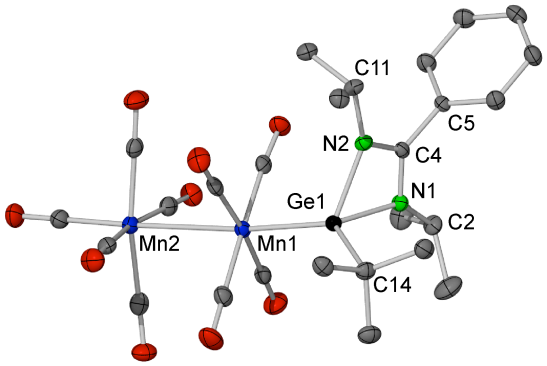

Figure 3. XRD molecular structure of **6** (40% displacement ellipsoids; H atoms omitted for clarity). Selected bond lengths (Å) and angles (deg): Mn1−Mn2 2.8565(7), Mn1−Ge1 2.3259(6), Ge1−C14 1.995(3), Ge1−N1 1.985(2), Ge1−N2 1.997(3), N1−C2 1.468(4), N1−C4 1.310(4), N2−C4 1.331(4), N2−C11 1.469(4), C4−C5 1.486(4); Mn1−Ge1−N1 120.16(8), Mn1−Ge1−N2 116.14(8), C14−Ge1−Mn1 127.5(1), C14−Ge1−N1 105.4(1), C14−Ge1−N2 104.8(1), N1−Ge1−N2 66.1(1), Ge1−N1−C4 92.0(2), Ge1−N2−C4 90.9(2), N1−C4−N2 110.8(3), Ge1−Mn1−Mn2 174.45(3).

Reactions of Complex 1 with Neutral 2-Electron-Donor Reagents. The reaction of germylene **A** with complex **1** in toluene at 90 °C afforded the CO-substituted derivative $[MnBr\{Ge(^iPr_2bzam)^tBu\}_2(CO)_3]$ (**7**) (Scheme 5). Its XRD structure (Figure 4) confirmed that the germylene ligands are *trans* to each other and *cis* to the bromido ligand and that the large steric bulk of germylene **A** impedes a *cis* arrangement of both germylenes. A similar *trans*-L_2-*mer*-$(CO)_3$

arrangement has been previously observed by XRD for $[MnBrL_2(CO)_3]$ complexes when L is a bulky phosphane (L = PCy_3, $P(p\text{-}ClC_6H_4)_3$).[19,20] However, a *cis*-L_2-*fac*-$(CO)_3$ structure has been observed when L is a small phosphane (L = $PPhH_2$, PPh_2H, PPh_2Me),[21–23] or an NHC (L = $I^iPr_2Me_2$ = 1,3-bis(isopropyl)-4,5-dimethylimidazol-2-ylidene).[24]

Scheme 5

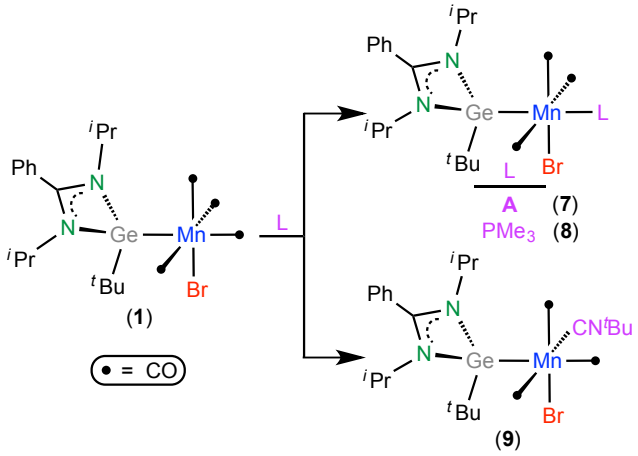

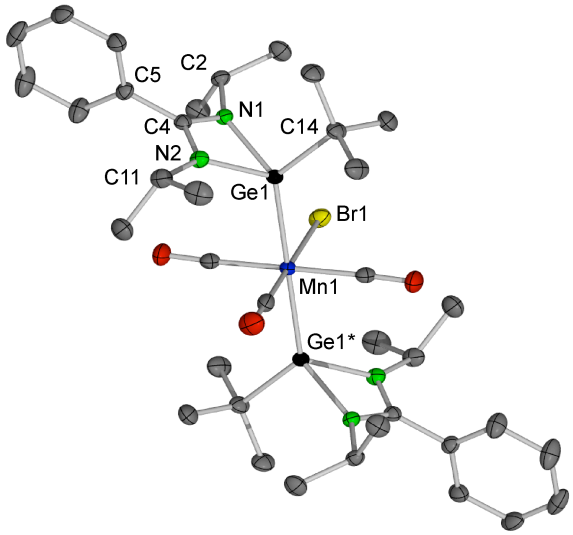

Figure 4. XRD molecular structure of **7** (40% displacement ellipsoids; H atoms omitted for clarity; the asymmetric unit contains one half of the molecule). Selected bond lengths (Å) and angles (deg): Mn1−Ge1 2.3533(2), Ge1−C14 2.009(2), Ge1−N1 2.002(1), Ge1−N2 1.999(2), N1−C2 1.469(2), N1−C4 1.318(3), N2−C4 1.331(2), N2−C11 1.458(3), C4−C5 1.490(2), Mn1−Ge1−N1 119.77(4), Mn1−Ge1−N2 119.91(4), C14−Ge1−Mn1 126.49(6), C14−Ge1−N1 104.51(7), C14−Ge1−N2 104.03(8), N1−Ge1−N2 66.07(7), Ge1−N1−C4 91.6(1), Ge1−N2−C4 91.4(1), N1−C4−N2 110.8(2), Ge1−Mn1−Ge1* 180.00. The Mn−Br distance is not given because the Br atom and its *trans* CO ligand are involved in exchange positional disorder (50:50 occupancy ratio).

As the above data suggested that, for $[MnBrL_2(CO)_3]$ complexes with small L ligands, the *cis*-L_2 arrangement is thermodynamically more stable than the *trans*-L_2 one, we decided to check this

reasoning by treating compound **1** with a small phosphane (PMe_3) and with an isonitrile (CN^tBu). Both reactions led to $[MnBrL\{Ge(^iPr_2bzam)^tBu\}(CO)_3]$ complexes (L = PMe_3 (**8**), CN^tBu (**9**)) (Scheme **5**). Interestingly, the pattern of the IR ν_{CO} absorptions of complex **8** is entirely analogous to that of complex **7**, but quite different from that of complex **9** (images of these IR spectra are provided in the Supporting Information). Therefore, complexes **7** and **8** are *mer*-tricarbonyl derivatives. An XRD study indicated that complex **9** has a *fac*-tricarbonyl structure (Figure 5). Subsequent DFT calculations (wB97XD/cc-pVDZ, SDD for Mn and Ge, level of theory) confirmed that the *fac*-tricarbonyl structure of $[MnBr(CN^tBu)\{Ge(^iPr_2bzam)^tBu\}(CO)_3]$ is 1.7 kcal mol^{-1} (Gibbs energy) more stable than the *mer*-tricarbonyl one. Hence, the large volume of germylene **A** hampers PMe_3 ligand to be *cis* to it, but it allows a linear CN^tBu ligand to be placed in this position.

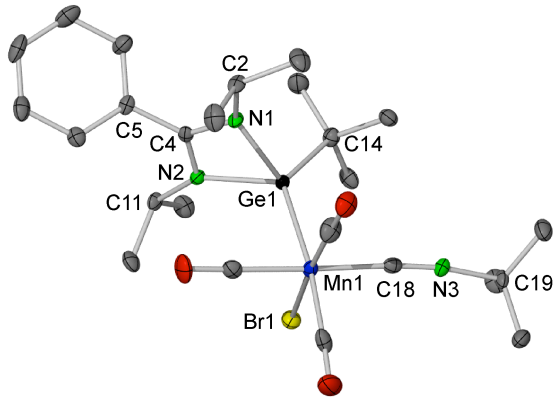

Figure 5. XRD molecular structure of **9** (60% displacement ellipsoids; H atoms omitted for clarity). Selected bond lengths (Å) and angles (deg): Mn1−Ge1 2.3958(8), Ge1−C14 2.009(5), Ge1−N1 1.988(4), Ge1−N2 2.001(4), N1−C2 1.465(6), N1−C4 1.337(5), N2−C4 1.339(5), N2−C11 1.468(5), C4−C5 1.488(6), Mn1−C18 1.936(5), C18−N3 1.159(6), C19−N3 1.466(5); Mn1−Ge1−N1 119.2(1), Mn1−Ge1−N2 116.9(1), C14−Ge1−Mn1 128.1(1), C14−Ge1−N1 103.4(2), C14−Ge1−N2 106.1(2), N1−Ge1−N2 66.5(1), Ge1−N1−C4 92.9(3), Ge1−N2−C4 91.5(3), N1−C4−N2 109.7(4), C18−N3−C19 170.7(4). The Mn−Br distance is not given because the Br atom and its *trans* CO ligand are involved in exchange positional disorder (93:7 occupancy ratio).

An interesting feature of the IR spectrum of complex **7** is that its ν_{CO} absorptions (toluene solution) are at much lower frequencies [1992 (w), 1911 (vs), 1873 (m) cm^{-1}] than those of complexes **8** [2009 (w), 1925 (vs), 1886 (m) cm^{-1}] and **9** [2013 (vs), 1954 (m), 1906 (m) cm^{-1}] and also than those reported for *mer*-$[MnBr(PCy_3)_2(CO)_3]$ [2015 (m), 1925 (s), 1885 (s) cm^{-1} in KBr][19] and *mer*-$[MnBr(P^iPr_3)_2(CO)_3]$ [2019 (w), 1932 (s), 1887 (m) cm^{-1}, in $CHCl_3$],[25] and *fac*-$[MnBr(I^iPr_2Me_2)_2(CO)_3]$ [2004, 1926, 1864 cm^{-1} (intensities not given), in C_6D_6].[24] Therefore, in line with previously reported results on the reactivity of germylene **A** with $[Ru_3(CO)_{12}]$,[11a] this germylene is a very strong electron-donating ligand, even stronger than the most basic trialkylphosphanes and N-heterocyclic carbenes.

Hydrolysis of Complex 1. Carrying out the above-described experiments, we noticed that the use of solvents that had not been carefully dried decreased the yields of the isolated products. Looking for a rationale to this observation we decided to treat complex **1** with water in dry toluene. The reaction, which was instantaneous at room temperature, led to $[^{i}Pr_2bzamH_2][MnBr\{Ge(OH)_2{}^{t}Bu\}(CO)_4]$ (**10**) (Scheme 6), which was isolated in 80% yield.

Scheme 6

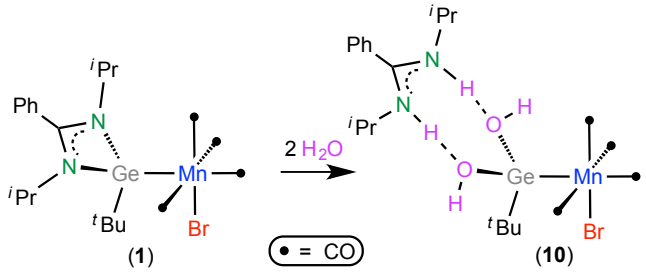

An XRD study (Figure 6) revealed that **10** is a salt that comprises $[^{i}Pr_2bzamH_2]^{+}$ benzamidinium cations and $[MnBr\{Ge(OH)_2{}^{t}Bu\}(CO)_4]^{-}$ complex anions. The anion is a bromidotetracarbonylmanganese(I) species that contains an unprecedented germanato(II) ligand, $[Ge(OH)_2{}^{t}Bu]^{-}$, in *cis* to the Br atom. Hydrogen bonding interactions are observed between the NH groups of the benzamidinium cation and the O atoms of the germanato ligand. The NH/OH protons were observed in the ^{1}H NMR spectrum as a very broad signal centered at 10.30 ppm (CD_2Cl_2, room temperature).

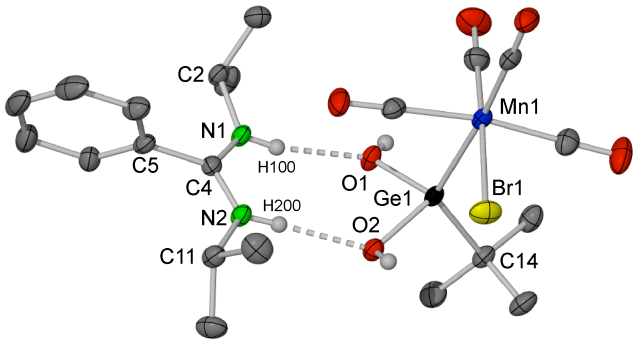

Figure 6. XRD structure of **10** (35% displacement ellipsoids; only one of the two analogous ionic pairs contained in the asymmetric unit is shown; H atoms omitted for clarity except those of the O–H and N–H groups). Selected bond lengths (Å) and angles (deg): Mn1–Ge1 2.4341(4), Mn1–Br1 2.5314(5), Ge1–C14 1.987(2), Ge1–O1 1.822(2), Ge1–O2 1.830(2), N1–C2 1.471(3), N1–C4 1.312(3), N2–C4 1.315(3), N2–C11 1.471(3), C4–C5 1.489(3), N1–H100 0.79(3), N2–H200 0.81(3), O1–H100 2.00(3), O2–H200 2.00(3); Mn1–Ge1–O1 112.05(6), Mn1–Ge1–O2 111.01(6), C14–Ge1–Mn1 126.76(7), C14–Ge1–O1 105.39(9), C14–Ge1–O2 103.16(9), O1–Ge1–O2 92.96(8), N1–C4–N2 120.3(2).

In a previous work, we observed that the hydrolysis of [Mn(OTf){Ge(^{i}Pr$_2$bzam)^{t}Bu}(CO)$_4$] (**2**) (Scheme 1), which is the OTf$^-$ version of **1**, led to a 1:2 mixture of the neutral binuclear oxodigermanato(II)-bridged complex [Mn$_2${μ-κ^4*Ge*$_2$*O*$_2$-OGe$_2$(OH)$_2$^{t}Bu$_2$}(CO)$_8$] and the amidinium salt [iPr$_2$bzamH$_2$]OTf.[4b] The isolation of **10** as the hydrolysis product of **1** suggests that an ionic derivative of formula [^{i}Pr$_2$bzamH$_2$][Mn(OTf){Ge(OH)$_2$^{t}Bu}(CO)$_4$] may be an intermediate in the formation of [Mn$_2${μ-κ^4*Ge*$_2$*O*$_2$-OGe$_2$(OH)$_2$^{t}Bu$_2$}(CO)$_8$] from [Mn(OTf){Ge(^{i}Pr$_2$bzam)^{t}Bu}(CO)$_4$] (**2**), since the release of [^{i}Pr$_2$bzamH$_2$]OTf from the former and the concomitant condensation of two resulting unsaturated units of [Mn{Ge(OH)$_2$^{t}Bu}(CO)$_4$] and the release of H$_2$O would lead to the final dimer. The fact that **10** is stable with respect to the release of [^{i}Pr$_2$bzamH$_2$]Br can be rationalized attending to the higher strength of the Mn–Br bond with respect to the Mn–OTf bond. Two additional reports have described hydrolytic degradations of amidinato-HT–TM complexes; [^{t}Bu$_2$bzamH$_2$]Cl has been obtained from reactions of coinage metal complexes containing the chlorogermylene Ge(^{t}Bu$_2$bzam)Cl,[4a] and the oxodigermylene-bridged derivative [Rh$_2$Cl$_2$(cod)$_2${μ-κ^2*Ge*,*Ge'*-OGe$_2$(tms$_2$bzam)$_2$}] (cod = 1,5-cyclooctadiene; tms = SiMe$_3$) has been obtained from the complex [RhCl(cod){Ge(tms$_2$bzam)$_2$}].[4c] In both cases, ionic pairs similar to **10** might be formed in the initial stages of the hydrolysis processes.

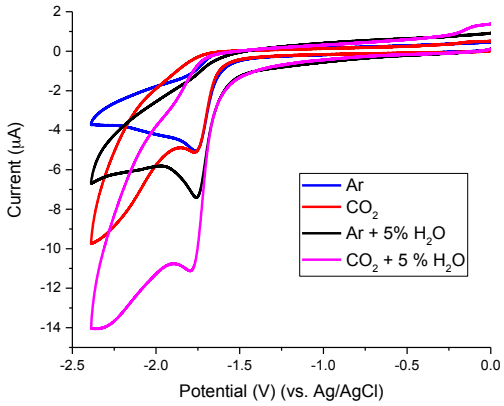

Figure 7. CVs at 0.2 V s^{-1} of a 1 mM solution of **10** in acetonitrile under Ar before (blue) and after (black) addition of 5 % H$_2$O, as well as under CO$_2$ before (red) and after (magenta) addition of 5 % H$_2$O.

The CV of **10** under argon in acetonitrile solution shows a single irreversible peak at –1.76 V (Figure 7). Noting that this value is less negative than that obtained with the mixture **1** + water in acetonitrile (see above), we tried to isolate the products of that reaction, but we were unable to isolate and characterize a well-defined complex. Therefore, the hydrolysis of **1** in acetonitrile is different from

that in toluene. Under CO_2 atmosphere, the first reduction of **10** is apparently not altered. However, the addition of water (5%) as Brønsted acid significantly increased the current peak of the first reduction, suggesting that complex **10** may catalyze the electrochemical reduction of CO_2 (Figure 7), in similar fashion as observed for [MnBr(bpy)$(CO)_3$]. It should be noticed that the addition of 5% of water to a solution of **10** under argon also has the effect to increase the CV current peak. With the aim to better quantifying the purported electrocatalytic activity of **10** in the presence of water, performed an exhaustive electrolysis at –1.90 V, monitoring the gas products by GC under a constant flow of CO_2 (8.67 mL min^{-1}), but, unfortunately, as observed in the case of **1**, at the end of the recorded time (103 min), the total TON of H_2 and CO produced were only 1.8 and 0.8, respectively.

CONCLUDING REMARKS

This contribution provides further insights into the reactivity (toward anionic and neutral nucleophiles) and catalytic applicability (for CO_2 electroreduction) of [MnBr{Ge(^{i}Pr$_2$bzam)^{t}Bu}$(CO)_4$] (**1**), which, prior to this work, was the only [MnBr$(CO)_5$]-derived complex to contain a heavier tetrylene ligand.

The reactions of **1** with LiPh and Li^{t}Bu led to dimer **5**. These reductive dimerization processes have been rationalized with the help of thermodynamic DFT calculations, which have also indicated that, for X = Br and OTf, the [MnX{Ge(^{i}Pr$_2$bzam)^{t}Bu}$(CO)_4$] complexes are more stable than the chelated derivatives [Mn{κ^2*N*,Ge-GeX(^{i}Pr$_2$bzam)^{t}Bu}$(CO)_4$]. The smaller volume of the Me group with respect to those of the Ph and ^{t}Bu groups, explain that, in the case of the reaction of **1** with LiMe, [Mn{κ^2*N*,Ge-GeMe(^{i}Pr$_2$bzam)^{t}Bu}$(CO)_4$] was the major product of a mixture that also contained some of **5**.

The reactions of **1** with neutral 2-electron donor reagents have unveiled that the coordination site of **1** implicated in CO-substitution reactions is strongly influenced by the large volume of the amidinatogermylene ligand, which induces a large germylene (**A**; complex **7**) and a rather small phosphane (PMe_3; complex **8**) to end in a coordination site *trans* to it, but it allows a linear CN^{t}Bu ligand to be placed *cis* to it (complex **9**). Remarkably, no germylene displacement has been observed in these reactions.

The hydrolysis of **1** in toluene solution led to a complex salt (compound **10**) that, in the solid state, features hydrogen bonding interactions between the NH groups of its benzamidinium cation and

the O atoms of an unprecedented κ*Ge*-alkyldihydroxogermanato(II) ligand. The structure of compound **10** sheds light on the process involved in the hydrolytic degradation of amidinato-HT–TM complexes.

Additionally, having in mind that various carbonyl manganese(I) complexes are catalytically active for the electroreduction of CO_2 to CO in the presence of Brønsted acids,[12] the electrochemical properties of complexes **1** and **10** were evaluated in presence of CO_2 in acetonitrile/H_2O solutions. Unfortunately, for both complexes, the catalytic production of CO was very small.

EXPERIMENTAL SECTION

General Procedures. Solvents were dried over appropriate desiccating reagents and were distilled under argon before use. All reactions were carried out under argon, using dry box and/or Schlenk-vacuum line techniques and were routinely monitored by solution IR spectroscopy. All reaction products were vacuum-dried for several hours prior to being weighted and analyzed. The germylene Ge(^{i}Pr$_2$bzam)^{t}Bu (**A**) and complex **1** were prepared following a published procedure.[7] All remaining reagents were purchased from commercial sources. NMR spectra were run on a Bruker DPX-300 instrument, using as standards a residual protic solvent resonance for ^{1}H [δ($C_6H D_5$) = 7.16 ppm; δ(CH_2Cl_2) = 5.32 ppm] and a solvent resonance for ^{13}C [δ(C_6D_6) = 128.1 ppm; δ(CH_2Cl_2) = 53.84 ppm]. Elemental analyses were obtained from a Perkin-Elmer 2400 microanalyzer. Mass spectra (MS) were run on a VG Autospec double-focusing mass spectrometer operating in the FAB+ mode; ions were produced with a standard Cs^+ gun at about 30 kV; 3-nitrobenzyl alcohol was used as matrix; data given correspond to the most abundant isotopomer of the molecular ion or of the greatest mass fragment.

[Mn$_2${Ge(^{i}Pr$_2$bzam)^{t}Bu}$_2$(CO)$_8$] (5): Method 1: LiPh (0.045 mL of a 1.8 M solution in dibutyl ether, 0.081 mmol) was added to a solution of complex **1** (42 mg, 0.072 mmol) in toluene (7 mL) at –78 ºC. The mixture was then allowed to reach the room temperature. An IR analysis of the solution (IR monitoring of ν_{CO} absorptions) showed a great amount of unreacted **1** and the formation of **5** as major reaction product. The complete consumption of **1** required the addition of additional 0.180 mL of LiPh solution (in several portions) and 3.5 h of stirring at room temperature. The initial yellow color changed to orange-red. The solvent was removed under reduced pressure and the crude reaction mixture was separated by column chromatography on silica-gel (2 x 5 cm). The major product, compound **5**, was eluted with hexane-dichloromethane (2:1) and was isolated after solvent removal as a

yellow solid (22 mg, 61 %). **Method 2:** Li^{t}Bu (0.045 mL of a 1.7 M solution in pentane, 0.077 mmol) was added to a solution of complex **1** (42 mg, 0.072 mmol) in toluene (7 mL) at –78 ºC. The mixture was then allowed to reach the room temperature. An IR analysis of the solution showed a great amount of unreacted **1** and the formation of **5** as major reaction product. The complete consumption of **1** (IR monitoring of ν_{CO} absorptions) required the addition of additional 0.090 mL of Li^{t}Bu solution (in several portions) and 2 h of stirring at room temperature. An analogous workup to that described above led to compound **5** (15 mg, 42%). **Method 3:** Germylene **A** (0.60 mL of a 0.25M solution in toluene, 0.150 mmol) was added to a solution of $[Mn_2(CO)_{10}]$ (29 mg, 0.074 mmol) in toluene (7 mL) and the mixture was heated at reflux temperature for 7 h. The initial yellow color changed to orange. An analogous workup to that described above led to compound **5** (15 mg, 20%). Anal. (%) Calcd. for $C_{42}H_{56}Ge_2Mn_2N_4O_8$ (FW = 1000.01 amu): C, 50.44; H, 5.64; N, 5.60; found: C, 50.46; H, 5.68; N, 5.57. (+)-FAB MS: *m/z* 1000 $[M]^+$. IR (toluene): ν_{CO} 1933 (s) cm^{-1}. ^{1}H NMR (C_6D_6, 300.1 MHz, 293 K): δ 7.12–6.60 (m, 5 H, Ph), 3.36 (sept, J = 7.0 Hz, 2 H, 2 C*H* of 2 ^{i}Pr), 1.41 (s, 9 H, ^{t}*Bu*), 1.24 (d, J = 7.0 Hz, 6 H, 2 *Me* of ^{i}Pr), 0.99 (d, J = 8.0 Hz, 6 H, 2 *Me* of ^{i}Pr) ppm. ^{13}C{^{1}H} NMR (C_6D_6, 100.6 MHz, 298 K): δ 169.2 (N*C*N), 138.0–122.1 (C_{ipso} + *C*Hs of 2 Ph), 47.5 (*C*H of 4 ^{i}Pr), 38.1 (*C* of ^{t}Bu), 26.4 (*Me*$_3$ of 2 ^{t}Bu), 24.4 (*Me* of 2 ^{i}Pr), 24.3 (*Me* of 2 ^{i}Pr) ppm (no ^{13}C resonances corresponding to the CO ligands were observed, even after long acquisition times).

[Mn$_2${Ge(*i*Pr$_2$bzam)*t*Bu}(CO)$_9$] (6): Germylene **A** (0.65 mL of a 0.08 M solution in toluene, 0.052 mmol) was added to a solution of $[Mn_2(CO)_{10}]$ (20 mg, 0.051 mmol) in toluene (5 mL) and the mixture was heated at reflux temperature for 4 h. The initial yellow color was maintained. The solvent was removed under reduced pressure and the residue was purified by column chromatography on silica-gel (2 x 5 cm). The major product, compound **6**, was eluted with hexane-dichloromethane (3:1) and was isolated after solvent removal as a yellow solid (25 mg, 71 %). Anal. (%) Calcd. for $C_{26}H_{28}GeMn_2N_2O_9$ (FW = 695.00 amu): C, 44.93; H, 4.06; N, 4.03; found: C, 44.97; H, 4.10; N, 4.00. (+)-FAB MS: *m/z* 696 $[M]^+$. IR (toluene): ν_{CO} 2080 (m), 1998 (m), 1980 (s), 1959 (w), 1921 (m) cm^{-1}. ^{1}H NMR (C_6D_6, 300.1 MHz, 298 K): δ 7.33–6.98 (m, 5 H, Ph), 3.22 (sept, J = 7.0 Hz, 2 H, 2 C*H* of 2 ^{i}Pr), 1.24 (s, 9 H, *Me*$_3$ of ^{t}Bu), 1.01 (d, J = 7.0 Hz, 6 H, 2 *Me* of 2 ^{i}Pr), 0.85 (d, J = 7.0 Hz, 6 H, 2 *Me* of 2 ^{i}Pr) ppm. ^{13}C{^{1}H} NMR (C_6D_6, 75.5 MHz, 298 K): δ 170.1 (N*C*N), 130.1 (C_{ipso} of Ph), 124.0–129.0 (*C*Hs of Ph), 47.6 (*C*H of 2 ^{i}Pr), 38.7 (*C* of ^{t}Bu), 26.0 (*Me*$_3$ of ^{t}Bu), 24.8 (*Me* of 2 ^{i}Pr), 24.0 (*Me* of 2 ^{i}Pr) ppm (no ^{13}C resonances corresponding to the CO ligands were observed, even after long acquisition times).

***Trans-mer*-[MnBr{Ge(^{i}Pr$_2$bzam)^{t}Bu}$_2$(CO)$_3$] (7):** Germylene **A** (0.40 mL of a 0.37 M solution in toluene, 0.148 mmol) was added to a solution of [MnBr(CO)$_5$] (20 mg, 0.073 mmol) and the mixture was heated at 90 ºC for 60 min. The initial yellow color changed to light orange. The solvent was removed under reduced pressure and the crude reaction mixture was purified by column chromatography on silica-gel (2 x 3 cm). Hexane-dicholoromethane (1:1) eluted compound **7**, which was isolated as a yellow solid (60 mg, 93 %). Anal. (%) Calcd. for $C_{37}H_{56}BrGe_2MnN_4O_3$ (FW = 884.93 amu): C, 50.22; H, 6.38; N, 6.33; found: C, 50.33; H, 6.41; N, 6.31. (+)-FAB MS: *m/z* 884 [*M*]$^+$. IR (toluene): ν_{CO} 1992 (w), 1911 (vs), 1873 (m) cm^{-1}. ^{1}H NMR (C_6D_6, 300.1 MHz, 293 K): δ 7.60 (m, 1 H, C*H* of Ph), 7.03 (m, 4 H, 4 C*H* of Ph), 3.52 (sept, *J* = 6.6 Hz, 2 H, 2 C*H* of 2 ^{i}Pr), 1.65 (s, 9 H, ^{t}*Bu*), 1.40 (d, *J* = 6.6 Hz, 6 H, 2 *Me* of ^{i}Pr), 1.22 (d, *J* = 6.6 Hz, 6 H, 2 *Me* of ^{i}Pr) ppm. ^{13}C{^{1}H} NMR (C_6D_6, 75.5 MHz, 293 K): δ 206.2 (*C*O), 224.5 (2 *C*Os), 170.0 (N*C*N), 131.1−127.7 (C_{ipso} + *C*Hs of Ph), 47.9 (2 *C*H of 2 ^{i}Pr), 38.5 (*C* of ^{t}Bu), 27.3 (*Me*$_3$ of ^{t}Bu), 25.2 (2 *Me* of 2 ^{i}Pr), 24.2 (2 *Me* of 2 ^{i}Pr) ppm.

***Trans-mer*-[MnBr(PMe$_3$){Ge(^{i}Pr$_2$bzam)^{t}Bu}(CO)$_3$] (8):** Germylene **A** (0.20 mL of a 0.37 M solution in toluene, 0.074 mmol) was added to a solution of [MnBr(CO)$_5$] (20 mg, 0.073 mmol) and the mixture was stirred at room temperature for 10 min. PMe$_3$ (7 µL, 0.080 mmol) was added and the mixture was heated at 70 ºC for 90 min. The initial yellow color changed to light orange. The solvent was removed under reduced pressure and the crude reaction mixture was purified by column chromatography on silica-gel (2 x 3 cm). Dichloromethane eluted compound **8**, which was isolated as a yellow solid (35 mg, 76 %). Anal. (%) Calcd. for $C_{23}H_{37}BrGeMnN_2O_3P$ (FW = 627.98 amu): C, 43.99; H, 5.94; N, 4.46; found: C, 44.03; H, 5.97; N, 4.41. (+)-FAB MS: *m/z* 544 [*M* – 3 CO]$^+$. IR (toluene): ν_{CO} 2009 (w), 1925 (vs), 1886 (m) cm^{-1}. ^{1}H NMR (C_6D_6, 300.1 MHz, 293 K): δ 7.48 (m, 1 H, C*H* of Ph), 7.03 (m, 4 H, 4 C*H* of Ph), 3.48 (sept, *J* = 6.6 Hz, 2 H, 2 C*H* of 2 ^{i}Pr), 1.56 (s, 9 H, ^{t}Bu), 1.38 (d, *J* = 8.8 Hz, 9 H, P*Me*$_3$), 1.33 (d, *J* = 6.6 Hz, 6 H, 2 *Me* of ^{i}Pr), 1.15 (d, *J* = 6.6 Hz, 6 H, 2 *Me* of ^{i}Pr) ppm. ^{13}C{^{1}H} NMR (C_6D_6, 75.5 MHz, 293 K): δ 225.1 (*C*O), 221.0 (2 *C*O), 170.3 (N*C*N), 130.7 (C_{ipso}), 130.0–127.5 (*C*Hs of Ph), 47.9 (2 *C*H of 2 ^{i}Pr), 38.3 (*C* of ^{t}Bu), 27.2 (*Me*$_3$ of ^{t}Bu), 25.2 (2 *Me* of 2 ^{i}Pr), 24.0 (2 *Me* of 2 ^{i}Pr), 18.2 (d, *J* = 27.9 Hz, P*Me*$_3$) ppm. ^{31}P{^{1}H} NMR (C_6D_6, 121.5 MHz, 293 K): δ 14.7 (s) ppm.

***Fac*-[MnBr(CN^{t}Bu){Ge(^{i}Pr$_2$bzam)^{t}Bu}(CO)$_3$] (9):** Germylene **A** (0.20 mL of a 0.37 M solution in toluene, 0.074 mmol) was added to a solution of [MnBr(CO)$_5$] (20 mg, 0.073 mmol) and the

mixture was stirred at room temperature for 10 min. CN^{t}Bu (9 μL, 0.080 mmol) was added and the mixture was heated at 70 ºC for 90 min. The initial yellow color changed to light orange. The solvent was removed under reduced pressure and the crude reaction mixture was purified by column chromatography on silica-gel (2 x 3 cm). Dicholoromethane eluted compound **9**, which was isolated as a yellow solid (29 mg, 63 %). Anal. (%) Calcd. for $C_{25}H_{37}BrGeMnN_3O_3$ (FW = 635.03 amu): C, 47.28; H, 5.87; N, 6.61; found: C, 47.12; H, 5.91; N, 6.57. (+)-FAB MS: *m/z* 551 $[M - 3\ CO]^+$. IR (toluene): ν_{CN} 2153 (w); ν_{CO} 2013 (vs), 1954 (m), 1906 (m) cm^{-1}. ^{1}H NMR (C_6D_6, 300.1 MHz, 293 K): δ 7.38 (m, 1 H, C*H* of Ph), 7.04 (m, 4 H, 4 C*H* of Ph), 3.59−3.32 (m, 2 H, 2 C*H* of 2 ^{i}Pr), 1.53 (s, 9 H, Ge^t*Bu*), 1.39 (d, *J* = 6.6 Hz, 3 H, *Me* of ^{i}Pr), 1.29 (d, *J* = 6.6 Hz, 3 H, *Me* of ^{i}Pr), 1.15 (d, *J* = 6.6 Hz, 3 H, *Me* of ^{i}Pr), 1.04 (s, 9 H, CN^t*Bu*), 1.03 (d, *J* = 6.6 Hz, 3 H, *Me* of ^{i}Pr) ppm. ^{13}C{^{1}H} NMR (C_6D_6, 75.5 MHz, 293 K): δ 224.0 (*C*O), 219.8 (*C*O), 216.7 (*C*O), 170.9 (N*C*N), 162.6 (*C*N^{t}Bu), 130.5−127.4 (C_{ipso} + *C*Hs of Ph), 57.5 (*C*Me$_3$ of CN^{t}Bu), 48.4 (*C*H of ^{i}Pr), 47.6 (*C*H of ^{i}Pr), 38.4 (*C* of ^{t}Bu), 30.2 (*Me*$_3$ of CN^{t}Bu), 27.5 (*Me*$_3$ of Ge^{t}Bu), 25.2 (*Me* of ^{i}Pr), 25.0 (*Me* of ^{i}Pr), 24.1 (*Me* of ^{i}Pr), 23.8 (*Me* of ^{i}Pr) ppm.

[^{i}Pr$_2$bzamH$_2$][MnBr{Ge(OH)$_2$^{t}Bu}(CO)$_4$] (10): Germylene **A** (0.20 mL of a 0.37 M solution in toluene, 0.074 mmol) was added to a solution of [MnBr(CO)$_5$] (20 mg, 0.073 mmol) and the mixture was stirred at room temperature for 10 min. Water (5 μL, 0.277 mmol) was added and the mixture was stirred at room temperature for 20 min. The initial yellow color changed to light orange. The solvent was removed under reduced pressure and the crude reaction mixture was purified by column chromatography on silica-gel (2 x 3 cm). Dichloromethane-THF (1:1) eluted compound **10**, which was isolated as a yellow solid (36 mg, 80 %). Anal. (%) Calcd. for $C_{21}H_{32}BrGeMnN_2O_6$ (FW = 615.94 amu): C, 40.95; H, 5.24; N, 4.55; found: C, 40.98; H, 5.29; N, 4.51. IR (toluene): ν_{CO} 2058 (m), 1983 (m), 1968 (vs), 1924 (m) cm^{-1}. ^{1}H NMR (CD_2Cl_2, 300.1 MHz, 293 K): δ 10.30 (s, vbr, N*H* + O*H*) 7.63−7.34 (m, 5 H, 5 C*H* of Ph), 3.25 (m, 2 H, 2 C*H* of ^{i}Pr), 1.23−1.19 (m, 21 H, *Me*$_3$ of ^{t}Bu + 4 *Me* of 2 ^{i}Pr) ppm. ^{13}C{^{1}H} NMR (CD_2Cl_2, 75.5 MHz, 293 K): δ 221.5 (CO), 217.8 (2 CO), 214.3 (CO), 164.5 (N*C*N), 132.0 (*C*H of Ph), 130.2 (2 *C*H of Ph), 126.9 (2 *C*H of Ph), 48.2 (2 *C*H of 2 ^{i}Pr), 35.5 (*C* of ^{t}Bu), 26.6 (*Me*$_3$ of ^{t}Bu), 23.1 (4 *Me* of 2 ^{i}Pr) ppm; the phenyl C_{ipso} resonance was not observed.

X-Ray Diffraction Analyses: Crystals of **5**, **6**, **7**, **9** and **10** were analyzed by X-ray diffraction. A selection of crystal, measurement, and refinement data is given in the Supporting Information (Table S1). Diffraction data were collected on an Oxford Diffraction Xcalibur Onyx Nova (**5**, **6**, **7**, and **10**) and on a Bruker CCD SMART1000 (**9**) single crystal diffractometers. Empirical absorption corrections

were applied using the SCALE3 ABSPACK algorithm as implemented in CrysAlisPro RED[26] (for **5**, **6**, **7** and **10**) and XABS2[27] (for **9**). The structures were solved using SIR-97.[28] Isotropic and full matrix anisotropic least square refinements were carried out using SHELXL.[29] All non-H atoms were refined anisotropically. Hydrogen atoms were set in calculated positions and refined riding on their parent atoms, except those of the O–H and N–H groups of **10**, which were located in a Fourier map. The asymmetric unit of **7** contains one manganese atom (0.5 occupancy) bonded to three groups disposed *cis* to each other, namely, one germylene ligand, one CO ligand and a third group that consists in a 50:50 occupancy ratio of CO and Br ligands (an inversion centre, the Mn atom, generates the whole molecule); therefore, in the crystal, the mutually *trans* Br and CO ligands, exchange their positions with a 50:50 occupancy ratio. Compound **9** also exhibits positional disorder involving the mutually *trans* Br and CO ligands, which exchange their positions with a 93:7 occupancy ratio. Restraints on the thermal and geometrical parameters of the atoms involved in the positional disorder of **9** were applied. The WINGX program system[30] was used throughout the structure determinations. The molecular plots were made with X-SEED.[31] CCDC deposition numbers: 1453071 (**5**), 1453072 (**6**), 1453073 (**7**), 1453074 (**9**) and 1453075 (**10**).

Electrochemical Studies: Cyclic voltammetry experiments were performed using a Metrohm Autolab 302N potentiostat, 1.0 mM solutions of the compounds in freshly distilled acetonitrile with tetrabutylammonium hexafluorophosphate as the supporting electrolyte (0.1 M). A single-compartment cell, having a glassy carbon (GC) working electrode (ø = 2 mm), a Pt counter electrode, and an Ag/AgCl (KCl 3 M) reference electrode, was employed. The Ar- and CO_2-saturated conditions were achieved by purging with the gases for 5 min before each potential sweep. A double compartment H-type cell was used for exhaustive electrolysis experiments, with a Pt wire as the counter electrode in a bridge separated from the cathodic compartment by a glass frit. A large surface glassy carbon rod (ø 2 cm) was used as the working electrode along with an aqueous Ag/AgCl (KCl 3M) reference electrode. A controlled flow of CO_2 (8.67 mL min^{-1}), measured just before arrival into the cell, was maintained during the exhaustive electrolysis measurements by means of a Smart Trak 100 (Sierra) flow controller, in a similar experimental setup as that previously described.[12c]

Computational Details: DFT calculations were carried out using the wB97XD functional,[32] which includes the second generation of Grimme's dispersion interaction correction[33] as well as long-range interactions effects. This functional reproduces the local coordination geometry of transition

metal compounds very well and it also corrects the systematic overestimation of non-bonded distances seen for all the density functionals not including estimates of dispersion.[34] The Stuttgart-Dresden relativistic effective core potentials and the associated basis sets (SDD) were used for the Mn[35] and Ge[36] atoms. The basis set used for the remaining atoms was the cc-pVDZ.[37] All stationary points were fully optimized in gas phase and confirmed as energy minima (all positive eigenvalues) by analytical calculation of frequencies. The electronic energies of the optimized structures were used to calculate the zero-point corrected energies and the enthalpic and entropic contributions via vibrational frequency calculations. Solvation free energies were obtained with the self-consistent reaction field (SCRF) for the standard continuum solvation model (CPCM),[38] by using the single-point solvation energy of the optimized structures and the thermodynamic correction from the gas phase calculations. All Gibbs energies were computed at 298.15 K and 1.0 atm. All calculations were carried out with the Gaussian09 package.[39] The atomic coordinates of all the DFT-optimized structures are given in the Supporting Information.

ASSOCIATED CONTENT

Supporting Information. X-ray crystallographic data in CIF format; crystal, acquisition, and refinement XRD data; atomic coordinates of DFT-optimized structures; ^{1}H and $^{13}C\{^{1}H\}$ NMR spectra; HOMO and LUMO of complex **1**; and complementary figures obtained from the electrochemical studies. This material is available free of charge via the Internet at http://pubs.acs.org.

AUTHOR INFORMATION

Corresponding Authors

*E-mails: jac@uniovi.es (J.A.C.), pga@uniovi.es (P.G.A.).

Author Contributions

The manuscript was written through contributions of all authors. All authors have given approval to the final version of the manuscript.

Notes

The authors declare no competing financial interest.

ACKNOWLEDGMENTS

This work has been supported by grants from MINECO-FEDER (CTQ2013-40619-P, MAT2013-40950-R, and RYC-2012-10491) and Gobierno del Principado de Asturias (GRUPIN14-009 and GRUPIN14-060).

REFERENCES

(1) For reviews on the synthesis and general chemistry of HTs, including transition metal coordination chemistry, see: (a) Marschner, C. *Eur. J. Inorg. Chem.* **2015**, 3805–3820. (b) Ghadwal, R. S.; Azhakar, R.; Roesky, H. W. *Acc. Chem. Res.* **2013**, *46*, 444–456. (c) Roesky, H. W. *J. Organomet. Chem.* **2013**, *730*, 57–62. (d) Asay, M.; Jones, C.; Driess, M. *Chem. Rev.* **2011**, *111*, 354–396. (e) Yao, S.; Xiong, Y.; Driess, M. *Organometallics* **2011**, *30*, 1748–1767. (f) Mandal, S. K.; Roesky, H. W. *Chem. Commun.* **2010**, *46*, 6016–6041. (g) Kira, M. *Chem. Commun.* **2010**, *46*, 2893–2903. (h) Nagendran, S.; Roesky, H. W. *Organometallics* **2008**, *27*, 457–492. (i) Zabula, A. V.; Hahn, F. E. *Eur. J. Inorg. Chem.* **2008**, 5165– 5179. (j) Leung, W.-P.; Kan, K.-W.; Chong, K.-H. *Coord. Chem. Rev.* **2007**, *251*, 2253–2265. (k) Kuhl, O. *Coord. Chem. Rev.* **2004**, *248*, 411–427. (l) Gehrhus, B.; Lappert, M. F. *J. Organomet. Chem.* **2001**, *617–618*, 209–223. (m) Haaf, M.; Schmedake, T. A.; West, R. *Acc. Chem. Res.* **2000**, *33*, 704–714. (n) Tokitoh, N.; Okazaki, R. *Coord. Chem. Rev.* **2000**, *210*, 251–277.

(2) For reviews focused on the transition metal coordination chemistry of HTs, see: (b) Cabeza, J. A.; García-Álvarez, P.; Polo, D. *Eur. J. Inorg. Chem.* **2016**, 10–22. (b) Álvarez-Rodríguez, L.; Cabeza, J. A.; García-Álvarez, P.; Polo, D. *Coord. Chem. Rev.* **2015**, *300*, 1–28. (c) Blom, B.; Gallego, D.; Driess, M. *Inorg. Chem. Front.* **2014**, *1*, 134–148. (d) Blom, B.; Stoelzel, M.; Driess, M. *Chem. Eur. J.* **2013**, *19*, 40–62. (e) Waterman, R.; Hayes, P. G.; Tilley, T. D. *Acc. Chem. Res.* **2007**, *40*, 712–719. (f) Okazaki, M.; Tobita, H.; Ogino, H. *Dalton Trans.* **2003**, 493–506. (g) Lappert, M. F.; Rowe, R. S. *Coord. Chem. Rev.* **1990**, *100*, 267–292. (h) Petz, W. *Chem. Rev.* **1986**, *86*, 1019–1047. (i) Lappert, M. F.; Power, P. P. *J. Chem. Soc., Dalton Trans.* **1985**, 51–57.

(3) For examples of oxidation processes on coordinated HTs, see: (a) York, J. T.; Young Jr., V. G.; Tolman, W. B. *Inorg. Chem.* **2006**, *45*, 4191–4198. (b) Cygan, Z. T.; Bender, J. E.; Litz, K. E.; Kampf, J. W.; Holl, M. M. B. *Organometallics* **2002**, *21*, 5373–5381. (c) Litz, K. E.; Holl, M. M. B.; Kampf, J. W.; Carpenter, G. B. *Inorg. Chem.* **1998**, *37*, 6461–6469.

(4) For examples of hydrolysis processes on coordinated HTs, see: (a) Álvarez-Rodríguez, L.; Cabeza, J. A.; García-Álvarez, P.; Polo, D. *Organometallics* **2015**, *34*, 5479−5484. (b) Cabeza, J. A.; García-Álvarez, P.; Pérez-Carreño, E.; Polo, D. *Inorg. Chem.* **2014**, *53*, 8735–8741. (c) Matioszek, D.; Saffon, N.; Sotiropoulos, J.-M.; Miqueu, K.; Castel, A.; Escudie, J. *Inorg. Chem.* **2012**, *51*, 11716–11721. (d) Zhanga, M.; Liua, X.; Shia, C.; Rena, C.; Dinga, Y.; Roesky, H. W. *Z. Anorg. Allg. Chem.* **2008**, *634*, 1755–1758. (e) Amoroso, D.; Haaf, M.; Yap, G. P. A.; West, R.; Fogg, D. E. *Organometallics* **2002**, *21*, 534–540. (f) Petri, S. H. A.; Eikenberg, D.; Neumann, B.; Stammler, H.-G.; Jutzi, P. P. *Organometallics* **1999**, *18*, 2615–2618. (g) Handwerker, H.; Leis, C.; Probst, R.; Bissinger, P.; Grohmann, A.; Kiprof, P.; Herdtweck, E.; Blumel, J.; Auner, N.; Zybill, C. *Organometallics* **1993**, *12*, 2162–6176. (h) Dostál, L.; Růžička, A.; Jambor, R. *Eur. J. Inorg. Chem.* **2014**, 5266–5270.

(5) For examples of displacement processes on coordinated HTs, see: (a) ref. 3a. (b) Evans, W. J.; Perotti, J. M.; Ziller, J. W.; Moser, D. F.; West, R. *Organometallics* **2003**, *22*, 1160–1163. (c) Herrmann, W. A.; Harter, P.; Gstottmayr, C. W. K.; Bielert, F.; Seeboth, N.; Sirsch, P. *J. Organomet. Chem.* **2002**, *649*, 141–146. (d) Yoo, H.; Carroll, P. J.; Berry, D. H. *J. Am. Chem. Soc.* **2006**, *128*, 6038–6039. (e) Probst, R.; Leis, C.; Gamper, S.; Herdtweck, E.; Zybill, C.; Auner, N. *Angew. Chem. Int. Ed. Engl.* **1991**, *30*, 1132–1135.

(6) Jones, C.; Rose, R. P.; Stasch, A. *Dalton Trans.* **2008**, 2871–2878.

(7) For amidinato-HT–TM complexes not included in review 2b, see: (a) ref. 4a. (b) Breit, N. C.; Szilvási, T.; Inoue, S. *Chem. Commun.* **2015**, *51*, 11272–11275. (c) Metsänen, T. T.; Gallego, D.; Szilvási, T.; Driess, M.; Oestreich, M. *Chem. Sci.* **2015**, *6*, 7143–7149.

(8) For examples of amidinato-HT−TM complexes as catalyst precursors, see: (a) ref. 7c. (b) Gallego, D.; Inoue, S.; Blom, B.; Driess, M. *Organometallics* **2014**, *33*, 5272–5282. (c) Gallego, D.; Inoue, S.; Blom, B.; Driess, M. *Organometallics* **2014**, *33*, 6885–6897. (d) Gallego, D.; Brück, A.; Irran, E.; Meier, F.; Kaupp, M.; Driess, M.; Hartwig, J. F. *J. Am. Chem. Soc.* **2013**, *135*, 15617–15626. (e) Blom, B.; Enthaler, S.; Inoue, S.; Irran, E.; Driess, M. *J. Am. Chem. Soc.* **2013**, *135*, 6703–6713. (f) Someya, C. I.; Haberberger, M.; Wang, W.; Enthaler, S.; Inoue, S. *Chem. Let.* **2013**, 42, 286–288. (g) Wang, W.; Inoue, S.; Enthaler, S.; Driess, M. *Angew. Chem. Int. Ed.* **2012**, *51*, 6167–6171. (h) Brück, A.; Gallego, D.; Wang, W.; Irran, E.; Driess, M.; Hartwig, J. F. *Angew. Chem. Int. Ed.* **2012**, *51*, 11478–11482.

(9) For studies showing the weaker nature of E–M bonds in HT-**T**M complexes in comparison with that of C–M bonds in NHC-TM complexes, see: (a) Nguyen, T. A. N.; Frenking, G. *Chem. Eur. J.* **2012**, *18*, 12733–12748. (b) Arp, H.; Baumgartner, J.; Marschner, C.; Zark, P.; Muller, T. *J. Am. Chem. Soc.* **2012**, *134*, 10864–10875. (c) Boehme, C.; Frenking, G. *Organometallics* **1998**, *17*, 5801–5809.

(10) For examples of $[MnXL_n(CO)_{5-n}]$ (X = halogen) complexes, see: (a) *Comprehensive Organometallic Chemistry*; Wilkinson, G., Stone, F. G. A., Abel, E. W., Eds.; Elsevier: Amsterdam, 1982; vol. 4 (Treichel, P. M., Ed.), pp 1–159. (b) *Comprehensive Organometallic Chemistry II*; Abel, E. W., Stone, F. G. A., Wilkinson, G., Eds.; Elsevier: Amsterdam, 1995; vol. 6 (Treichel, P. M., Ed.), pp 1–19. (c) *Comprehensive Organometallic Chemistry III*; Crabtree, R. H., Mingos, D. M. P., Eds.; Elsevier: Amsterdam, 2007; vol. 5 (Sweigart, D. A., Reingold, A. J., Son, S. U., Eds.), pp 761–813.

(11) See, for example: (a) Álvarez-Rodríguez, L.; Cabeza, J. A.; García-Álvarez, P.; Pérez-Carreño, E.; Polo, D. *Inorg. Chem.* **2015**, *54*, 2983–2994. (b) Cabeza, J. A.; Fernández-Colinas, J. M.; García-Álvarez, P.; Pérez-Carreño, E.; Polo, D. *Inorg. Chem.* **2015**, *54*, 4850–4861. (c) Cabeza, J. A.; García-Álvarez, P.; Pérez-Carreño, E.; Polo, D. *Chem.–Eur. J.* **2014**, *20*, 8654–8663. (d) Cabeza, J. A.; Fernández-Colinas, J. M.; García-Álvarez, P.; Polo, D. *RSC Adv.* **2014**, *4*, 31503–31506.

(12) (a) Franco, F.; Cometto, C.; Ferrero Vallana, F.; Sordello, F.; Priola, E.; Minero, C.; Nervi, C.; Gobetto, R. *Chem. Commun.* **2014**, *50*, 14670–14673. (b) Bourrez, M; Molton, F.; Chardon-Noblat, S.; Deronzier, A. *Angew. Chem. Int. Ed.* **2011**, *50*, 9903–9906. (c) Franco, F.; Cometto, C.; Sordello, F.; Minero, C.; Nencini, L.; Fiedler, J.; Gobetto, R.; Nervi, C. *ChemElectroChem* **2015**, *2*, 1372–1379. (d) Machan, C. W.; Sampson, M. D.; Chabolla, S. A.; Dang, T.; Kubiak, C. P. *Organometallics* **2014**, *33*, 4550–4559. (e) Zeng, Q.; Tory, J.; Hartl, F. *Organometallics* **2014**, *33*, 5002–5008. (e) Vollmer, M. V.; Machan, C. W.; Clark, M. L.; Antholine, W. E.; Agarwall, J.; Schaefer III, H. F.; Kubiak, C. F.; Walensky, J. R. *Organometallics* **2015**, *34*, 3–12. (f) Agarwall, J.; Shaw, T. W.; Schaefer III, H. F.; Bocarsly, A. B. *Inorg. Chem.* **2015**, *54*, 5285–5294. (g) Machan, C. W.; Stanton III, C. J.; Vandezande, J. E.; Majetich, G. F.; Schaefer III, H. F.; Kubiak, C. F.; Agarwall, J. *Inorg. Chem.* **2015**, *54*, 8849–8856. (h) Agarwall, J.; Shaw, T. W.; Stanton III, C. J.; Majetich, G. F.; Bocarsly, A. B.; Schaefer III, H. F. *Angew. Chem. Int. Ed.* **2014**, *53*, 5152–5155.

(13) Decken, A.; MacKay, A. J.; Brown, M. J.; Bottomley, F. *Organometallics* **2002,** *21,* 2006–2009.

(14) Gismondi. T. E.; Rausch, M. D. *J. Organomet. Chem.* **1985**, *284*, 59–71.

(15) (a) Meunier-Piret, J.; van Meerssche, M.; Gielen, M.; van den Eynde, I. *Bull. Soc. Chem. Belg.* **1984**, *93*, 307–312. (b) Laing, M.; Absworth, T.; Sommerville, P.; Singleton, E.; Reinmann, R. *Chem. Commun.* **1972**, 1251–1251. (c) Masuda, H.; Taga, T.; Sowa, T.; Kawamura, T.; Yonezawa, T. *Inorg. Chim. Acta* **1985**, *101*, 45–48. (d) Hunt, J. J.; Duesler, E. N.; Paine, R. T. *J. Organomet. Chem.* **1987**, *320*, 307–315. (e) Decken, A.; Nell, M. A.; Bottomley, F. *Can. J. Chem.* **2001**, *79*, 1321–1321. (f) Eischenbroich, C.; Six, J.; Hams, K. *Chem. Commun.* **2006**, 3429–3431. (g) Herberhold, M.; Milius, W.; Pfeifer, A. *Z. Naturforsch.* **2003**, *58b*, 1–10. (h) Karmaker, S.; Ghosh, S.; Kabir, S. E.; Haworth, D. T.; Lindeman, S. V. *Inorg. Chim. Acta* **2012**, *382*, 199–202. (i) Munchenberg, J.; Fischer, A. K.; Thonnessen, H.; Jones, P. G.; Schmutzier, R. *J. Organomet. Chem.* **1997**, *529*, 361–374. (j) Bennett, M. J.; Mason, R. *J. Chem. Soc. A* **1968**, 75–81.

(16) (a) Azhakar, R.; Roesky, H. W.; Holstein, J. J.; Dittrich, B. *Dalton. Trans.* **2012**, *41*, 12096–12100. (b) Azhakar, R.; Sarish, S. P.; Roesky, H. W.; Hey, J.; Stalke, D. *Inorg. Chem.* **2011**, *50*, 5039–5043.

(17) (a) Kabir, S. E.; Ahmed, F.; Gosh, S.; Hassan, M. R.; Islam, M. S.; Sharmin, A.; Tocher, D. A.; Haworth, D. T.; Lindeman, S. V.; Siddiquee, T. A.; Bennett, D. W.; Hardcastle, K. I. *J. Organomet. Chem.* **2008**, *693*, 2657–2665. (b) Henrick, K.; McPartlin, M.; Iggo, J. A.; Kemball, A. C.; Mays, M. J.; Raithby, P. R. *J. Chem. Soc., Dalton Trans.* **1987***,* 2669–2682. (c) Hor, T. S. A.; Chan, H. S. O.; Tan, K.-L.; Phang, L.-T.; Yan, Y. K. *Polyhedron* **1991***, 10*, 2437–2450. (d) Laing, M.; Singleton, E.; Reinmann, R. *J. Organomet. Chem.* **1973**, *56*, C21–C22. (e) Florke, U.; Haupt, H.-J. *Z. Kristallogr.* **1998**, *213*, 267–XXX. (f) Florke, U.; Haupt, H.-J. *Z. Kristallogr.* **1990**, *191*, 153–155. (g) Decken, A.; Bottomley, F.; Wilkins, B. E.; Gill, E. D. *Organometallics* **2004***, 23*, 3683–3693.

(18) (a) Giorgano, R.; Sappa, E.; Tiripicchio, A.; Tiripicchio-Camellini, M. T.; Mays, M. J.; Brown, M. P. *Polyhedron* **1989**, *8*, 1855–1856. (b) Meijboom, R.; Dhirori, P.; Mavunkai, I. J. *Inorg. Chim. Acta* **2009**, *362*, 617–620.

(19) Toupadakis, A.; Kubas, G. J.; King, W. A.; Scott, B. L.; Huhmann-Vincent, J. *Organometallics* **1998**, *17*, 5315–5323.

(20) Beckett, M. A.; Brassington, D. S.; Coles, S. J.; Light, M. E.; Hursthouse, M. B. *J. Organomet. Chem.* **2003**, *688*, 174–180.

(21) Pope, S. J. A.; Reid, G. *J. Chem. Soc., Dalton Trans.* **1999**, 1615–1622.

(22) Manzoni de Oliveira, G.; Horner, M.; Seiffert, M.; Bortoluzzi, A. J. *J. Chem. Cryst.* **1999**, *29*, 193–197.

(23) Germán-Acacio, J. M.; Reyes-Lezama, M.; Zúñiga-Villarreal, N. *J. Organomet. Chem.* **2006**, *691*, 3223–3231.

(24) Martin, T. A.; Ellul, C. E.; Mahon, M. F.; Warren, M. E.; Allan, D.; Whittlesey, M. K. *Organometallics* **2011**, *30*, 2200–2211.

(25) Kuchynka, D. J.; Amatore, C.; Kochi, J. K. *J. Organomet. Chem.* **1987**, *328*, 133–154.

(26) *CrysAlisPro RED,* version 1.171.34.36: Oxford Diffraction Ltd.: Oxford, UK, 2010.

(27) Parkin, S.; Moezzi, B.; Hope, H. *J. Appl. Cryst.* **1995**, *28*, 53–56.

(28) Altomare, A.; Burla, M. C.; Camalli, M.; Cascarano, G. L.; Giacovazzo, C.; Guagliardi, A.; Moliterni, A. G. C.; Polidori, G.; Spagna, R. *J. Appl. Crystallogr.* **1999**, *32*, 115–119.

(29) *SHELXL-2014*: Sheldrick, G. M. *Acta Crystallogr.* **2008**, *A64*, 112–122.

(30) *WINGX*, version 1.80.05 (2009*)*: Farrugia, L. J. *J. Appl. Crystallogr.* **1999**, *32*, 837–838.

(31) X-Seed: Barbour, L. J. *J. Supramol. Chem.* **2001,** *1*, 189–191.

(32) Chai, J.-D.; Head-Gordon, M. *Phys. Chem. Chem. Phys.* **2008**, *10*, 6615–6620.

(33) (a) Ehrlich, S.; Moellmann, J.; Grimme, S. *Acc. Chem. Res.* **2013**, *46*, 916–926. (b) Grimme, S. *Comp. Mol. Sci.* **2011**, *1*, 211–228. (c) Schwabe, T.; Grimme, S. *Acc. Chem. Res.* **2008**, *41*, 569–579.

(34) Minenkov, Y.; Singstad, Å; Occhipinti, G.; Jensen, V. R. *Dalton Trans.* **2012**, *41*, 5526–5541.

(35) Dolg, M.; Wedig, U.; Stoll, H.; Preuss, H. *J. Chem. Phys.* **1987**, *86*, 866–872.

(36) Bergner, A.; Dolg, M.; Kuechle, W.; Stoll, H.; Preuss, H. *Mol. Phys.* **1993**, *80*, 1431–1441.

(37) Dunning, T. H. *J. Chem. Phys.* **1989**, *90*, 1007–1023.

(38) (a) Barone, V.; Cossi, M. *J. Phys. Chem. A* **1998**, *102*, 1995–2001. (b) Cossi, M.; Rega, N.;

Scalmani, G.; Barone, V. *J. Comput. Chem.* **2003**, *24*, 669–681.

(39) Frisch, M. J.; Trucks, G. W.; Schlegel, H. B.; Scuseria, G. E.; Robb, M. A.; Cheeseman, J. R.; Scalmani, G.; Barone, V.; Mennucci, B.; Petersson, G. A.; Nakatsuji, H.; Caricato, M.; Li, X.; Hratchian, H. P.; Izmaylov, A. F.; Bloino, J.; Zheng, G.; Sonnenberg, J. L.; Hada, M.; Ehara, M.; Toyota, K.; Fukuda, R.; Hasegawa, J.; Ishida, M.; Nakajima, T.; Honda, Y.; Kitao, O.; Nakai, H.; Vreven, T.; Montgomery, J. A., Jr.; Peralta, J. E.; Ogliaro, F.; Bearpark, M.; Heyd, J. J.; Brothers, E.; Kudin, K. N.; Staroverov, V. N.; Kobayashi, R.; Normand, J.; Raghavachari, K.; Rendell, A.; Burant, J. C.; Iyengar, S. S.; Tomasi, J.; Cossi, M.; Rega, N.; Millam, N. J.; Klene, M.; Knox, J. E.; Cross, J. B.; Bakken, V.; Adamo, C.; Jaramillo, J.; Gomperts, R.; Stratmann, R. E.; Yazyev, O.; Austin, A. J.; Cammi, R.; Pomelli, C.; Ochterski, J. W.; Martin, R. L.; Morokuma, K.; Zakrzewski, V. G.; Voth, G. A.; Salvador, P.; Dannenberg, J. J.; Dapprich, S.; Daniels, A. D.; Farkas, Ö.; Foresman, J. B.; Ortiz, J. V.; Cioslowski, J.; Fox, D. J. *Gaussian 09*, revision A.01; Gaussian, Inc.: Wallingford, CT, 2009.

TOC Graph